ELSEVIER

Contents lists available at ScienceDirect

Colloids and Surfaces A: Physicochemical and Engineering Aspects

journal homepage: www.elsevier.com/locate/colsurfa



Simultaneous removal of Cd(II) and 2-chlorophenol from aqueous solution using activated carbon supported titanate nanotubes



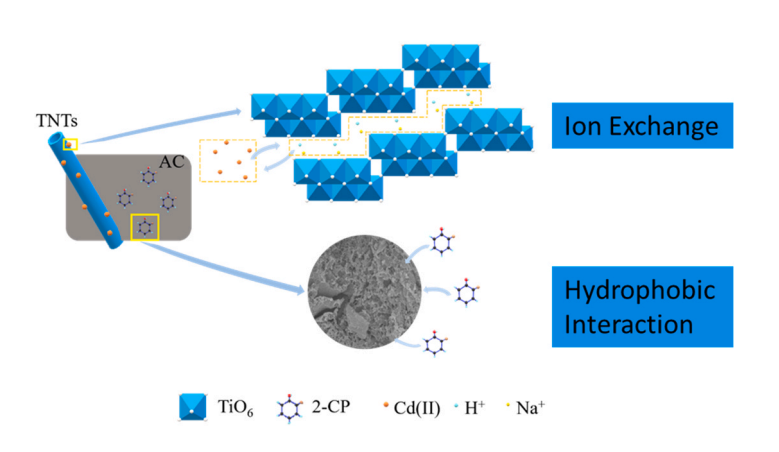
Xianping Deng^a, Peiwen Wu^a, Xiaodong Du^a, Guining Lu^a, Yanyan Gong^{b,*}, Zhi Dang^{a,c,**}, Dongye Zhao^{d,*}

- ^a School of Environment and Energy, South China University of Technology, Guangzhou 510006, China
- ^b School of Environment, Guangdong Key Laboratory of Environmental Pollution and Health, Jinan University, Guangzhou 511443, China
- ^c The Key Lab of Pollution Control and Ecosystem Restoration in Industry Clusters, Ministry of Education, South China University of Technology, Guangzhou 510006, China
- d Department of Civil, Construction and Environmental Engineering, San Diego State University, San Diego, CA 92182-1324, USA

HIGHLIGHTS

- A carbon-titanate composite TNTs@AC can simultaneously adsorb Cd(II) and 2-CP
- Cd(II) ions are bound to titanate nanotubes via ion exchange.
- 2-CP is adsorbed the activated carbon phase via hydrophobic interaction.
- The simultaneous adsorption of Cd(II) and 2-CP on TNTs@AC is independent.
- Carbon-TNTs mixed phases are promising for simultaneous removal of metals and organics.

GRAPHICAL ABSTRACT



ARTICLE INFO

Keywords: Cd(II) 2-chlorophenol Activated carbon Titanate nanotube Simultaneous removal Composite material

ABSTRACT

Combined heavy metals and chlorinated organic compounds have been widely reported in industrial wastewater. Yet, simultaneous removal of these contaminants remains challenging. In this study, a bi-functional composite (TNTs@AC) was prepared based on commercial titanium dioxide (TiO₂) and activated carbon (AC) and tested for simultaneous removal of Cd(II) and 2-chlorophenol (2-CP). Under the action of high temperature and pressure, TiO_2 was transformed into titanate nanotubes (TNTs) and bound to AC, and in the meanwhile, nanoscale AC particles were patched on the TNTs. In the mixed TNTs and AC phases, TNTs was responsible for taking up Cd(II), whereas AC for 2-CP. As such, the relative adsorption capacities of the composite for Cd(II) and 2-CP varied with the mass ratio of TiO_2 :AC, with decent uptakes for both chemicals in the mass ratio rage of 1:3 \sim 1:1. TNTs@AC (prepared at TiO_2 :AC = 1:1) demonstrated fast sorption kinetics and high sorption capacities for both Cd(II) and 2-CP, with a maximum Langmuir adsorption capacity of 109 and 52 mg/g, respectively, in the single solute

^{*} Corresponding authors.

^{**} Corresponding author at: School of Environment and Energy, South China University of Technology, Guangzhou 510006, China. *E-mail addresses*: yanyangong@jnu.edu.cn (Y. Gong), chzdang@scut.edu.cn (Z. Dang), dzhao2@sdsu.edu (D. Zhao).

systems. In the binary systems, the adsorption capacity of Cd(II) was not affected by the presence of 2-CP, whereas the presence of Cd(II) slightly increased the uptake of 2-CP in the low Cd concentration domain (final Cd $< 7 \, \text{mg/L}$) but mildly inhibited the uptake at Cd $> 7 \, \text{mg/L}$. The dominant adsorption mechanism of Cd (II) was ion exchange between Cd(II) and Na $^+$ /H $^+$ of the -ONa/H group of TNTs; while AC served as the primary sink for 2-CP via hydrophobic interaction along with some other possible mechanisms such as surface complexation and hole filling. TNTs@AC also performed well under common environmental conditions (pH, common co-ions, and dissolved organic matter). The formation of mixed TNTs and AC microphases appears promising for simultaneous removal of heavy metals and organic compounds from contaminated water.

1. Introduction

With the rapid industrial development, water pollution by heavy metals and organic pollutants has become a major environmental concern [1–4]. Anthropogenic activities including leather, paint, dye, pharmaceutical, paper, textile printing, and dveing industry can result in widespread water contamination of heavy metals and organic compounds [2,5,6]. Cadmium, Cd(II), has been one of the most commonly detected heavy metals. Exposure to Cd can lead to kidney damage, emphysema, hypertension, cardiovascular disease, diabetes, and bone deformity [7]. Likewise, chlorophenol (CP) has also been detected in industrial wastewater and exposure to CP has been associated with the disorder of cell bilayer phospholipid structure, carcinogenesis, and mutagenesis [2,8]. As Cd and CP have been found often co-present in industrial wastewater, the toxicity of such combined pollutants was feared to be far greater than the sum of individual pollutants [5,6,9]. Therefore, there is an urgent need for treatment technologies or materials that can simultaneously remove both metal cations and organic pollutants like Cd(II) and CP.

Adsorption has been widely practiced for removal of heavy metals and organic pollutants from water [10,11]. While most work has been shooting for only one type of pollutants (metals or organics), researchers have also explored simultaneous removal of mixture of heavy metals and organic pollutants. For instance, Andini et al. [12] investigated simultaneous adsorption of chlorobenzene and Pb2+ and Cd(II) using organophilic bentonite, and they observed that in the single-solute systems, organophilic bentonite showed much higher adsorption capacity for chlorophenol (maximum capacity = 700 mg/g) over Pb^{2+} (22 mg/g) and Cd(II) (2.8 mg/g). However, when the metals and chlorophenol were co-present, the adsorption was mutually inhibitive, and the capacity of chlorophenol was reduced to 0.3 g/g, while nearly no adsorption was observed for the metals. Deng et al. [7] investigated simultaneous adsorption of Cd(II) and ionic dyes by a magnetic graphene oxide nanocomposite. In the single solute systems, the maximum sorption capacities for Cd(II), methylene blue (MB) and orange G (OG) were 91.29, 64.23, and 20.85 mg/g, respectively. However, when MB and Cd(II) were co-present, the adsorption of Cd(II) was reduced from 91.29 to 21.38 mg/g. As such, dual-functional sorbents that can effecively remove both 2-chlorophenol (2-CP) and Cd(II) in multicomponent systems are needed.

For sorption of hydrophobic organic pollutants, activated carbon (AC) is generally the first choice [13–15] because of its low cost, commercial availability, and adsorption properties. However, AC is not effective for adsorption of metal cations due to its very limited cation exchange capacity, and thus, special modification of AC has been explored [14]. In recent years, titanate nanotubes (TNTs) synthesized from TiO_2 have attracted extensive attention due to their high sorption capacity on various metal cations and photocatalytic properties [16–18]. Like AC, researchers have explored various ways to modify TNTs to enhance adsorption or photocatalysis properties [19,20].

Considering AC's excellent adsorption ability for hydrophobic organic pollutants and TNTs's ability to take up metal cations, we postulated that combining AC and TNTs in such a way that can form a mixed AC-TNTs microphases (i.e., the two materials can be composited at the microscale) will result in a new composite material that can

adsorb both organics and metal cations concurrently. The concept was first proven by Duan et al. [20], who synthesized activated carbon fiber (ACF) supported/modified TNTs (TNTs/ACF). Combining the advantages of TNTs and ACF, TNTs/ACF showed synergistic adsorption of U (VI) and 2-CP in the binary system. However, compared with AC, ACF is not only more expensive, but has smaller specific surface area and thus lower adsorption capacity [21,22]. Therefore, combining AC and TNTs may lead to a dual-functional sorbent (TNTs@AC), which can efficiently remove both Cd(II) and 2-CP from water under typical environmental conditions. To the best of our knowledge, simultaneous removal of Cd (II) and 2-CP using TNTs@AC has not been explored.

The overall goal of this study was to prepare, optimize and test a dual functional sorbent (TNTs@AC) for simultaneous removal of both Cd(II) and 2-CP from aqueous solution. The specific objectives were to (1) prepare and characterize TNTs@AC based on commercial TiO_2 and AC through a one-step hydrothermal process, (2) test the effectiveness of TNTs@AC for simultaneous removal of Cd(II) and 2-CP, (3) elucidate the underlying removal mechanisms, and (4) explore the effects of environmental conditions, namely, pH, co-existing ions, and humic acid (HA) on the removal of Cd(II) and 2-CP.

2. Materials and methods

2.1. Materials

Filtrosorb-400 granular AC (F-400 GAC) was acquired from Calgon Carbon Corporation (Pittsburgh, PA, USA). Nano-TiO $_2$ (P25, ca. 80% anatase and 20% rutile), cadmium nitrate tetrahydrate (Cd(NO $_3$) $_2$ -4 H $_2$ O), and ethanol (C $_2$ H $_5$ O) were purchased from Aladdin Reagents Co., Ltd. (Shanghai, China). Humic acid (HA) and 2-chlorophenol (2-CP) were obtained from Shanghai Macklin Biochemical Co., Ltd (Shanghai, China). Sodium chloride (NaCl), Calcium chloride (CaCl $_2$), and sodium hydroxide (NaOH) were bought from General-Reagent (Shanghai, China). Sodium nitrate (NaNO $_3$) and nitric acid (HNO $_3$) were acquired from Guangzhou Chemical Reagent Factory (Guangzhou, China). Sodium dihydrogen phosphate (NaH $_2$ PO $_4$) was from Comeio Chemical Reagent Co., Ltd. (Tianjin, China). Methanol (HPLC grade) was from CNW Company (Shanghai, China). Deionized (DI) water (18.2 M $_2$ Cm) was used in this work.

2.2. Preparation of TNTs@AC

TNTs@AC was synthesized via a modified one-step hydrothermal approach [20]. In brief, $1.2~g~TiO_2$ and 1.2~g~AC (100 mesh) were added into 66.7 mL of 10 M NaOH solution, and the mixture was continuously stirred in a plastic beaker for 12 h. The evenly dispersed mixture was then transferred to a 100 mL Teflon lined stainless steel reactor and reacted at 130 °C for 72 h. The resultant gray-black material was washed thoroughly with DI water to remove the residual alkaline solution and impurities. Finally, the composite was dried at 80 °C for 4 h and sieved through a 100 mesh to obtain particles with size less than 0.15 mm.

To test the effect of the AC: TiO_2 mass ratio, TNTs@AC was prepared at five AC: TiO_2 mass ratios, namely, 3:1, 2:1, 1:1, 1:2 and 1:3. For comparison, single AC and TNTs, which represented a AC: TiO_2 mass ratio of 1:0 and 0:1, respectively, were also prepared under otherwise

identical conditions.

was measured using a TOC analyzer with a detection limit of 0.2 mg/L.

2.3. Characterization

The structure and surface morphology of TNTs@AC were analyzed by scanning electron microscope (SEM, Merlin, Carl Zeiss AG, Germany), transmission electron microscope (TEM) and energy dispersive spectrometer (EDS, Escalab Xi+, Thermo Fisher Scientific, USA). The specific surface area and pore size were measured following the multipoint N_2 -BET adsorption approach (Autosorb iQ, Anton Paar, Shanghai, China). The crystallinity was characterized by X-ray diffractometer (XRD, Empyrean, PANalytical B.V., Netherlands). The surface functional groups were analyzed by (FTIR, iS50, Thermo Fisher Scientific, USA), The elemental composition was identified via X-ray photoelectron spectroscopy (XPS, Escalab Xi+, Thermo Fisher Scientific, USA).

2.4. Batch adsorption experiments

Batch adsorption kinetic tests were carried out to test the material performance in single-solute and binary systems, and all test were performed using 150 mL amber glass bottles and at 25 °C. Based on the reported concentrations of Cd(II) and 2-CP in industrial wastewater, we set their initial concentrations to 10 mg/L and 5 mg/L, respectively [23, 24]. The adsorption was initiated by mixing 7 mg of TNTs@AC with 100 mL a solution containing Cd(II) and/or 2-CP at an initial pH of 7.0 \pm 0.1. The bottles were then sealed and agitated at 165 rpm on a horizontal shaker for 6 h. At predetermined time intervals, 2 mL sample was taken and immediately filtered through a 0.22 μm membrane filter (PTFE), and the concentration of Cd(II) or 2-CP in the filtrates was then analyzed. Following the screening experiments, the best performed TNTs@AC (prepared at the best AC:TiO2 ratio) was further studied.

The uptake $(q_t, mg/g)$ of Cd(II) and 2-CP at time t is calculated by [25]:

$$q_t = \frac{(C_0 - C_t)V}{m}$$
 (1)

where C_0 and C_t (mg/L) are the concentrations of Cd(II) or 2-CP at time 0 and t, respectively, V (L) is the solution volume, and m (g) is the mass of TNTs@AC.

The adsorption isotherms of Cd(II) or 2-CP were constructed in both single-solute and binary systems following the similar procedure at in the kinetic tests. TNTs@AC dosage was 70 mg/L, the reaction pH was kept constant at 7.0 ± 0.1 , and the equilibration time was 6 h. For Cd (II), the initial concentration of Cd(II) ranged from 5 to 70 mg/L, without 2-CP (single solute) or in the presence of 5 mg/L 2-CP (binary system). For 2-CP, the initial concentration of 2-CP ranged from 2 to 20 mg/L, with 0 or 10 mg/L Cd(II). Control tests showed that the adsorption of Cd(II) or 2-CP on the bottles or during the sample processing was negligible. All experiments were conducted in duplicate and the results are reported as mean \pm relative deviation from the mean.

To test the effects of environmental conditions, the adsorption equilibrium experiments were also carried out at pH ranging from 2 to 11, co-existing ionic (Na $^+$, Ca $^{2+}$, Cl $^-$, NO $_3$, H $_2$ PO $_4$) from 0 to 10 mM, and HA from 0 to 10 mg/L.

2.5. Analytical methods

Cd(II) was analyzed using AAS (PinAAcle 900 T, Perkin Elmer, Guangzhou, China) and the detection limit was 0.01 mg/L. 2-CP was measured via a HPLC system (Agilent 1200, NYSE: A, Palo Alto, USA) equipped with a UV detector and a C18 column (Agilent Eclipse Plus C18, 4.6×150 mm \times 5 μm). The mobile phase consists of 60% methanol and 40% water. The injection volume was 20 μL and the mobile phase flow rate was 0.8 mL/min. The UV wavelength was set at 274 nm. The detection limit of 2-CP was 0.025 mg/L. Total organic carbon (TOC)

3. Results and discussion

3.1. Characterization

Fig. 1 shows the SEM and TEM images of AC and TNTs@AC. While the plain AC exhibited a bulky, smooth, and flat surface (Fig. 1a), TNTs@AC displayed a much rougher surface with aggregated clusters or a network of TNTs (Fig. 1b). A close-up of the TNTs@AC surface shows the tubular TNTs that are interwoven and blended with fine carbon microparticles (Fig. 1c). The TEM image (Fig. 1d) further confirmed TNTs-decorated AC and revealed a tube diameter of ~10 nm for the TNTs. The EDS spectra (Fig. S1 in Supporting Material (SM)) revealed four elements, C, O, Na, and Ti on the TNTs@AC surface, which were rather uniformly distributed (Fig. S2).

Fig. 2 shows the XRD patterns of TNTs@AC before and after the reaction with Cd(II) or 2-CP. For neat TNTs@AC, the peaks at 9.6°, 24.4°, 28.2° and 48.3° are attributed to sodium trititanate [19,22,26, 27]. Moreover, the peaks at 9.6° represents the interlayer distance (crystal plane (200)) of sodium trititanate [26,28]. The peak at 25.9° represents graphite carbon, confirming that AC particles are intermingled with TNTs.[26] Upon Cd(II) or 2-CP uptake, the characteristic peaks of sodium trititanate at 9.6°, 24.4°, 28.2° and 48.3° remained. However, for Cd(II)-laden TNTs@AC, the characteristic peak at 9.8° was weakened, indicating a larger interlayer spacing [16]. For neat TNTs@AC, the exchangeable interlayer counter ions were H⁺ and/or Na⁺ [26]. Upon Cd(II) uptake, Cd(II) ions were taken up in exchange with the H⁺ of -OH and/or Na⁺ ions on TNTs@AC[16,29], resulting in the larger interlayer spacing. Other characteristic peaks did not change significantly, indicating that the Cd(II) adsorption did not change the octahedral skeleton of TNTs@AC. Upon 2-CP uptake, no significant change was observed in the XRD pattern, indicating that the adsorption of 2-CP did not affect the crystalline properties of the composite.

Fig. 3 compares the N₂ adsorption-desorption isotherms and pore size distributions of TNTs, 1:2 TNTs@AC and 1:1 TNTs@AC (The number indicates the initial TiO₂:AC mass ratio). All the three materials showed type IV isotherm with the H4 hysteresis loop indicating the mesoporous structures [30–32]. It was reported that the specific surface area of AC (F-400) was 1069.2 m²/g, and 80% of the surface area was situated in pores of < 2 nm (diameter) [33]. TNTs displayed a bimodal pore size distribution profile with a primary peaking at 3.8 nm and a secondary peaking at 5.6 nm, and the dominant pore size was mesoporous. These pores were derived from the pores inside titanate nanotubes, whose inner diameter was equal to the pore size [29]. 1:2 TNTs@AC also showed a bimodal pore size distribution profile with a primary peaking at 2.8 nm and a secondary peaking at 3.8 nm, and the dominant pore size was mesoporous, and no micropore structure smaller than 2 nm was detected, which can be due to the blockage during the material synthesis. 1:1 TNTs@AC has a wider pore size range (2–50 nm), and the dominant pore size was around 3.9 nm, while a small portion of 5.9, 7.4, 8.4 and 19 nm pore sizes were also observed. The pore size larger than 10 nm was derived from the meso-pore formed by the stacking of AC and TNTs. The specific surface area of TNTs is $133.42 \text{ m}^2/\text{g}$.

Based on the measured specific surface areas of AC (1069.2 m^2/g) and TNTs (133.42 m^2/g) (Table S1), the specific surface areas of 1:2 TNTs@AC and 1:1 TNTs@AC were calculated to be 757.27 and 601.31 m^2/g , respectively. If they were combined without distortion. The measured specific surface areas were 575.28 and 456.34 m^2/g (Table S1), which are lower than the theoretical values, indicating partial blockage the interior pores during the alkaline hydrothermal treatment.

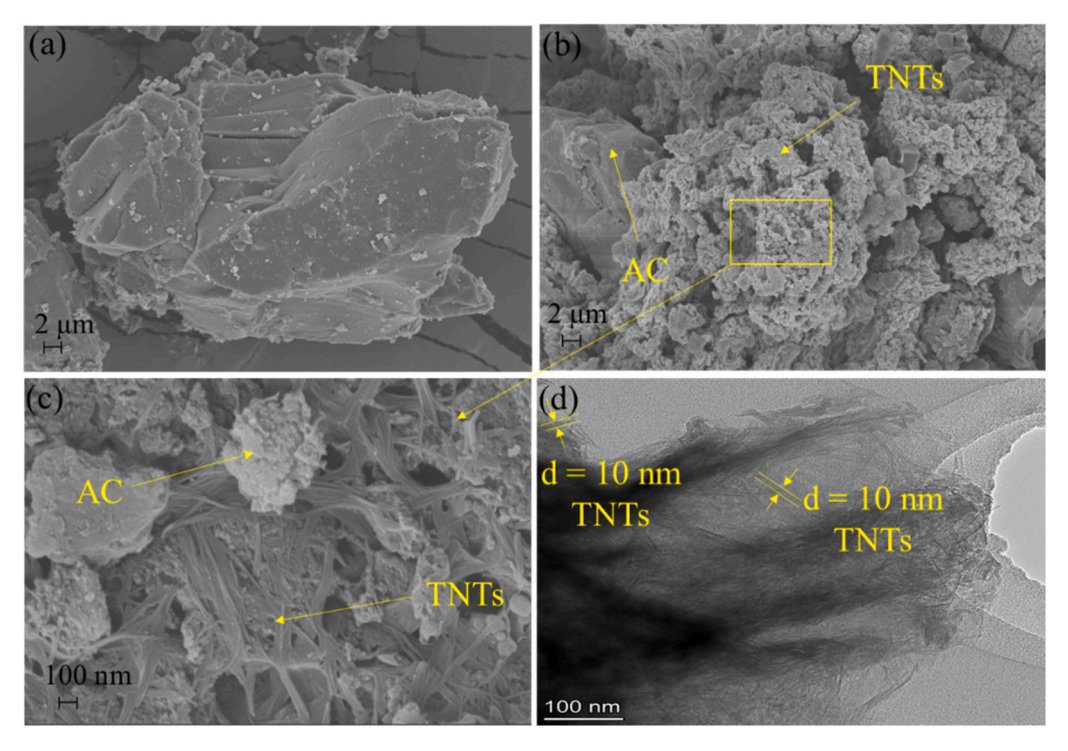
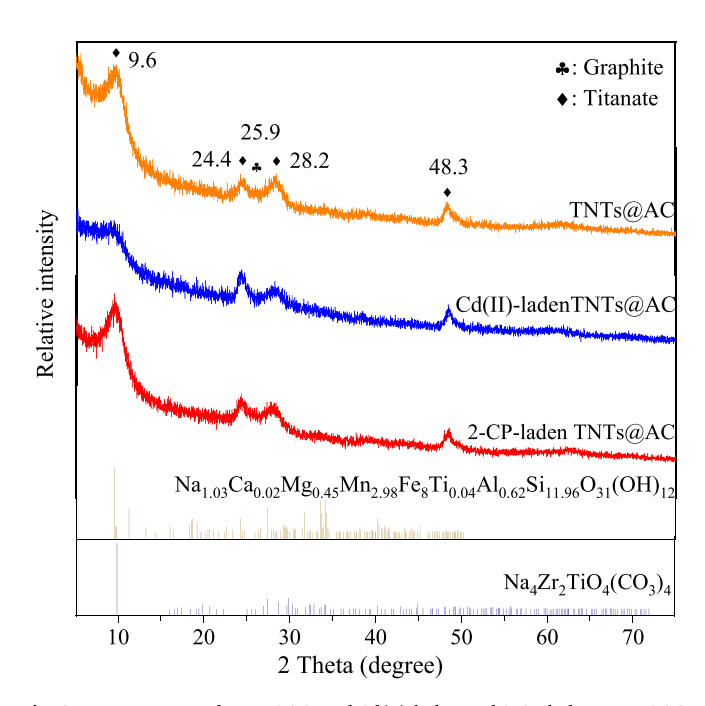


Fig. 1. SEM images of (a) AC and (b, c) TNTs@AC, and (d) TEM images of TNTs@AC.



 $\textbf{Fig. 2.} \ \ \textbf{XRD patterns of TNTs@AC}, and \ \textbf{Cd(II)-laden and 2-CP-laden TNTs@AC}.$

3.2. Effect of TiO2:AC mass ratio on Cd(II) and 2-CP adsorption

Fig. 4 compares the equilibrium uptakes of Cd(II) and 2-CP by TNTs@AC prepared at various TiO_2 :AC mass ratios in the binary systems. The plain AC only removed 2-CP, with an equilibrium uptake of 78.9 mg/g, while TNTs only removed Cd(II) with an uptake of 142 mg/g. When the TiO_2 :AC mass ratio was increased from 1:3 to 3:1, the 2-CP uptake decreased from 60.0 to 14.1 mg/g, while the Cd(II) uptake elevated from 57.3 to 139.0 mg/g.

The results agree with the perception that the adsorption of 2-CP was facilitated by the AC phase via hydrophobic interactions, whereas the

uptake of Cd(II) was mainly by the TNTs phase via electrostatic interactions [20]. With the increasing TiO₂:AC mass ratio, the specific surface area of the composite decreased and some of the AC sites were blocked due to the patching and blocking effects of TNTs, leading to the decreasing adsorption of 2-CP. In contrast, elevating the portion of TNTs on the surface resulted in the growing uptake of Cd(II). Considering a balanced sorption capacity, TNTs@AC prepared at the TiO₂:AC ratio of 1:1 was further studied in the subsequent experiments. Apparently, in practical applications, the ratio can be adjusted according to the relative contents of Cd(II) and 2-CP (or metals versus organics at large).

3.3. Adsorption kinetics

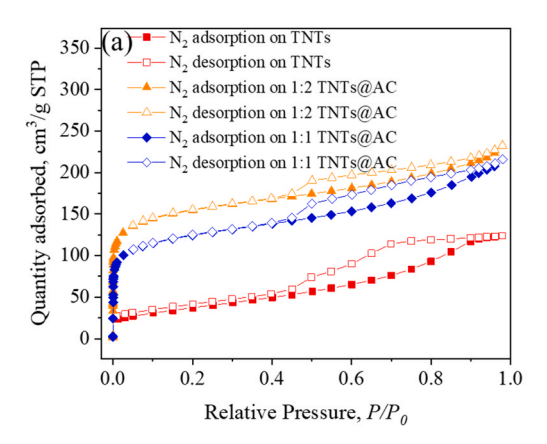
Adsorption kinetic tests were conducted to determine the removal rates of Cd(II) and 2-CP by TNTs@AC in both single-solute and binary systems (Fig. 5). For all cases, the adsorption displayed a rapid intial rate in the first 40 min and then slowed down, and the gradual adsorption appeared to continue after 300 min for Cd(II) and 360 min for 2-CP. This phenomenon is consistent with the common notion that more accessible adsorption sites are occupied first [34]. Yet, the very gradual second stage adosprtion suggests that some very slow diffusion in micromores is likely limiting the adsorption in the late stage. In the single-solute systems, the final uptakes of Cd(II) and 2-CP reached 113 and 40 mg/g, respectively. In the binary system, the uptake of Cd(II) was not affected by the presence of 2-CP, but the adsorption of 2-CP was increased by 7.5% in the presence of Cd(II), suggesting that the adsorption of Cd(II) faciliated the uptake of 2-CP.

The adsorption kinetic data of Cd(II) and 2-CP were interpreted using the pseudo first-order (Eq. 2) and the pseudo second-order (Eq. 3) kinetic models: [20].

$$q_t = q_e - q_e \exp(-k_1 t) \tag{2}$$

$$q_t = \frac{k_2 q_e^2 t}{1 + k_2 q_e t} \tag{3}$$

where $k_1 \,(\text{min}^{-1})$ and $k_2 \,(\text{g mg}^{-1} \,\text{min}^{-1})$ are the rate constants of the two kinetic models, respectively, and q_e is the equilibrium adsorption of Cd



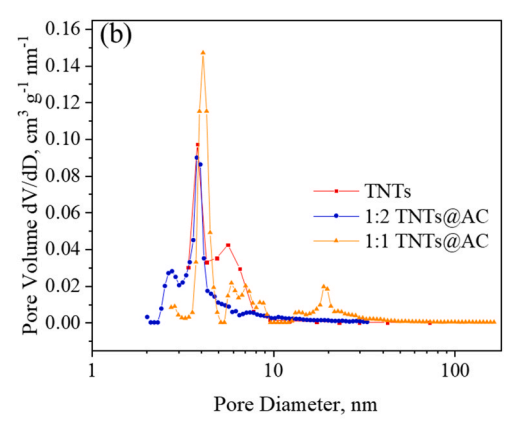


Fig. 3. (a) N_2 adsorption-desorption isotherms, and (b) pore size distributions of TNTs, 1:2 TNTs@AC, and 1:1 TNTs@AC.

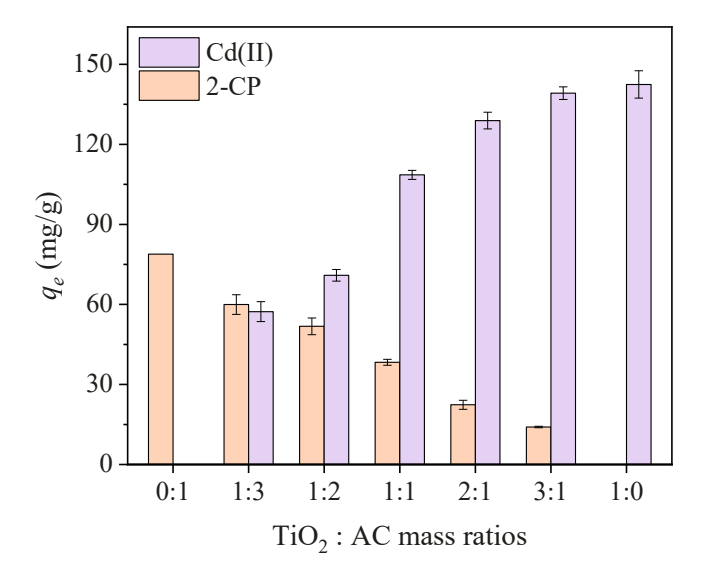


Fig. 4. Effects of on Cd(II) and 2-CP removal. Experimental conditions: initial concentration of Cd(II) = 10 mg/L, 2-CP = 5 mg/L, material dosage = 70 mg/L, pH = 7.0 ± 0.1 in binary solute system. q_e refers to equilibrium adsorption capacity of Cd(II) and 2-CP, and reaction time = 6 h.

(II) or 2-CP.

Table 1 summarizes the best-fitted parameters of the kinetics models. The pseudo second-order kinetic model ($R^2=0.937$ –0.995) provided better fitting of the experimental data than the pseudo first-order kinetic model ($R^2=0.899$ –0.962) in all cases. The calculated equilibrium

uptakes (q_e) using the pseudo second-order kinetic model were 115 and 40 mg/g for Cd(II) and 2-CP, respectively, which are close to the values at the end of the kinetic experiments. The k_2 values for Cd(II) are 9.9×10^{-4} and 7.0×10^{-4} g mg⁻¹ min⁻¹, respectively, in the single and binary systems, and those for 2-CP are 0.0014 and 0.0024 (g mg⁻¹ min⁻¹). In the binary solute systems, the rate constants were comparable for Cd(II) and 2-CP. Therefore, when the two pollutants are absorbed synchronously, their adsorption rates will not change.

3.4. Adsorption isotherms

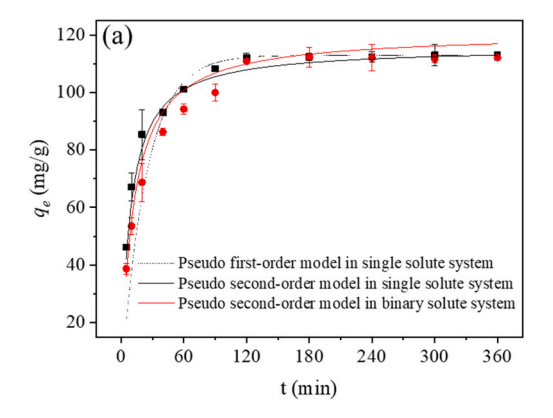
Fig. 6 shows the adsorption isotherms of Cd(II) and 2-CP by TNTs@AC in the single-solute and binary systems. The Langmuir, Freundlich[35] and dual-mode [20] isotherm models are applied to fit the isotherm data:

Langmuir model :
$$q_e = \frac{q_{\text{max}} K_L C_e}{1 + K_L C_e}$$
 (4)

Freundlich model :
$$q_e = K_F C_e^{1/n}$$
 (5)

$$Dual - mode \ model: q_e = \frac{q_{max} K_L C_e}{1 + K_L C_e} + K_d C_e$$
 (6)

where q_e (mg/g) is the equilibrium uptake, C_e (mg/L) is the solute concentration at equilibrium, q_{max} (mg/g) is the maximum monolayer capacity of the adsorbent, K_L (L/mg) is the Langmuir adsorption constant, which is related to the affinity of adsorption, K_F (mg/g·(L/mg)^{1/n}) is the Freundlich adsorption isotherm coefficient, n is the Freundlich exponent, which is related to the intensity of adsorption, K_d is the distribution coefficient (L/g). The classical Langmuir model assumes that



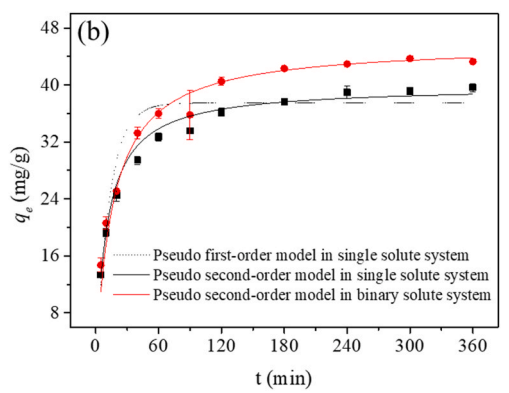


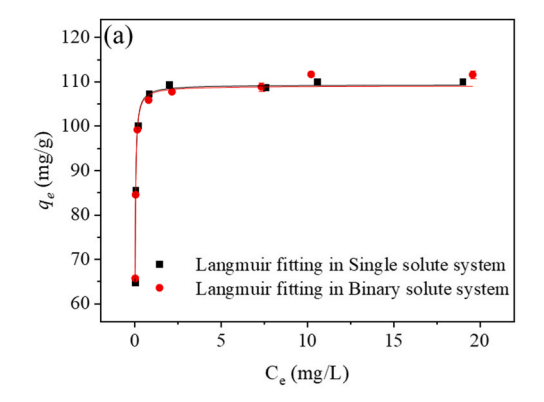
Fig. 5. Sorption kinetics of (a) Cd(II) and (b) 2-CP by TNTs@AC in the single and binary solute systems. Experimental conditions: initial concentration of Cd(II) = 10 mg/L, initial concentration of 2-CP = 5 mg/L, material dosage = 70 mg/L, and pH = 7.0 ± 0.1 .

Table 1
Best-fitted parameters of the pseudo first-order model and pseudo second-order models for adsorption of Cd(II) and 2-CP by TNTs@AC in single and binary solute systems.

Kinetic models	Parameters	Single solute system		Binary solute system	
		Cd (II)	2-CP	Cd (II)	2-CP
	k_1 (min ⁻¹)	0.042 ± 0.0033	0.044 ± 0.0023	0.041 ± 0.0052	0.044 ± 0.0023
Pseudo					
first-order	$q_{\mathrm{e,1}}~(\mathrm{mg/g})$	112 ± 0.322	43 ± 0.24	111 ± 1.03	43 ± 0.24
kinetic model					
	R^2	0.899	0.980	0.923	0.981
	$k_2 (\mathrm{min}^{-1})$	0.00099 ± 0.000039	0.0024 ± 0.00016	0.0007 ± 0.0001	0.0014 ± 0.000062
Pseudo second-order kinetic model	$q_{\mathrm{e,2}}$ (mg/g)	115 ± 0.139	40 ± 0.24	121 ± 2.05	46 ± 0.19
	R^2	0.994	0.994	0.937	0.995
	$q_{\rm e,exp}$ (mg/g)	113 ± 0.015	40 ± 0.55	112 ± 0.753	43 ± 0.19

k1 and k2 are the respective rate constants of the pseudo first and second order kinetic models.

 $q_{\rm e,exp}$ is the experimental equilibrium uptake.



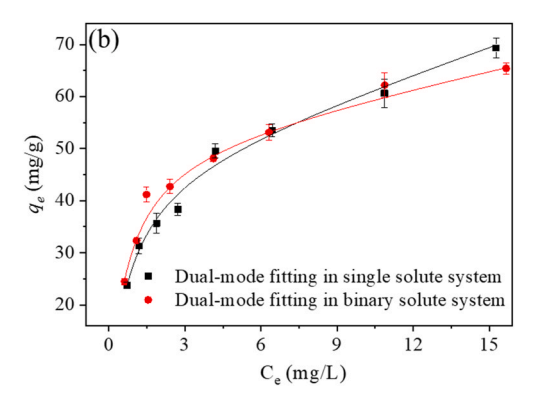


Fig. 6. Sorption isotherms of (a) Cd(II) and (b) 2-CP by TNTs@AC in the single and binary solute systems. Experimental conditions: initial concentration of Cd(II) = 5–70 mg/L, initial concentration of 2-CP = 2–20 mg/L, material dosage = 70 mg/L, pH = 7.0 \pm 0.1, and temperature = 25 \pm 1 °C, and reaction time = 6 h.

adsorption is homogeneous and monolayer and that there is no interaction between adsorbates. Freundlich model assumes heterogeneous adsorption and is an empirical equation [35]. Dual-mode model is composed of a Langmuir-type adsorption term and a linear accumulation or participation term [20].

Table 2 gives the resultant model parameters. In the single-solute system, the Langmuir model gave the best goodness of fitting ($R^2=0.999$) of the Cd(II) isotherm, and the maximum adsorption capacity of Cd(II) was 109 mg/g. The results were consistent with previous studies that the adsorption mechanism of TNTs for metal cations is ion exchange [16,36]. In contrast, the dual mode model gave the best goodness of fitting ($R^2=0.985$) for the 2-CP isotherm, and the maximum monolayer adsorption capacity was 47.6 mg/g. The results suggest that the adsorption of 2-CP not only involved hydrophobic interaction on the surface of activated carbon, but also some other mechanisms such as multilayer accumulation and/or capillary condensation in the AC-nanoparticles-modified TNTs.[37].

In the binary systems, the Langmuir model again gave the best fitting $({\rm R}^2=1.00)$ of the Cd(II) data, and the maximum capacity was 109 mg/g. It can be seen that the Langmuir fitting parameters of Cd in the binary solute system were almost the same as those in single solute system, and there was no significant difference through t-test. This is also consistent with the kinetic data. For the sorption of 2-CP, the dual mode model gave the best fitting (${\rm R}^2=0.991$), and the maximum adsorption capacity being 52 mg/g. The influence of Cd(II) on the adsorption of 2-CP was dependent of the concentration of 2-CP. In the presence of 10 mg/L Cd (II), the equilibrium uptake of 2-CP was slightly increased (by up to 15.7%) when the initial concentration of 2-CP was higher. The co-

Table 2Isotherm model parameters for sorption of Cd(II) and 2-CP by TNTs@AC in single and binary solutes systems.

Sorption		Single solute system		Binary solute system	
isotherm models	Parameters	Cd (II)	2-CP	Cd (II)	2-CP
	$q_{\rm max}$ (mg/g)	109 ± 0.574	67 ± 4.0	109 ± 0.160	64 ± 2.8
Langmuir	b (L/mg)	$65 \\ \pm 0.87$	$\begin{array}{c} 0.71 \\ \pm \ 0.12 \end{array}$	$64 \\ \pm 0.24$	$\begin{array}{c} 0.92 \\ \pm \ 0.12 \end{array}$
model	R^2	0.999	0.947	1.00	0.959
	$K_F (mg/g \cdot (L/mg)^{1/n})$	$109 \\ \pm 7.79$	$\begin{array}{l} 28 \\ \pm \ 0.77 \end{array}$	$\begin{array}{c} 135 \\ \pm \ 18.5 \end{array}$	31 ± 1.0
Freundlich model	n	$\begin{array}{c} 0.14 \\ \pm \ 0.020 \end{array}$	$\begin{array}{c} 0.35 \\ \pm \ 0.017 \end{array}$	$\begin{array}{l} 0.19 \\ \pm \ 0.037 \end{array}$	$\begin{array}{l} 0.28 \\ \pm \ 0.020 \end{array}$
model	R^2	0.814	0.983	0.720	0.963
	K_d (L/g)		$\begin{array}{c} 1.6 \\ \pm \ 0.37 \end{array}$		$1.0 \\ \pm 0.21$
Dual-mode	$q_{\rm max} ({\rm mg/g})$		48 ± 4.1		52 ± 2.6
model	b (L/mg)		1.3		1.4
			± 0.23		± 0.17
	R^2		0.985		0.991

qmax is the maximum Langmuir adsorption capacity.

b is the Langmuir affinity constant.

 K_F and n are the Freundlich model capacity constant and exponent, respectively. K_d is the distribution coefficient.

adsorption of Cd(II) may have slightly opened up the TNTs structure or offered some additional surface complexation between Cd and the phenolic group. On the other hand, the sorbed Cd(II) rendered a more hydrophilic surface and may have block some of the AC sites, resulting in

 $q_{\mathrm{e},1}$ and $q_{\mathrm{e},2}$ are equilibrium uptake from the first and second order models.

the reduced uptake of 2-CP at elevated 2-CP concentration.

3.5. Adsorption mechanisms of Cd(II) and 2-CP by TNTs@AC

Fig. 7 shows FTIR spectra of TNTs@AC before and after reaction with Cd(II) and/or 2-CP. For neat TNTs@AC, three characteristic peaks at 3243, 1629 and 881 cm⁻¹ represent the O-H vibration from hydroxyl group, H-O-H vibration from bounded water molecules, and a fourcoordinated Ti-O(TiO(OH)2) vibration involving nonbridging oxygen atoms that are coordinated with Na ions, respectively [18,20,29,31,38]. Upon 2-CP uptake, the H-O-H vibration shifted from 1629 to 1622 cm⁻¹ which was due to the vibration of the aromatic ring bonding of 2-CP [20]. In addition, the peak representing O-H vibration near 3243 cm⁻¹ before adsorption split into two new peaks at 3250 and 3334 cm⁻¹ after adsorption, which is characteristic of the phenolic -OH.[20,39] Other characteristic peaks were almost unchanged, indicating that 2-CP is adsorbed on the material surface through hydrophobic interaction and will not change the material structure and properties. Upon Cd(II) uptake, the Ti-O(TiO(OH)2) vibration involving nonbridging oxygen atoms at $881~\text{cm}^{-1}$ disappeared due to ion exchange of the Na $^+$ in TNTs@AC with Cd(II), which is also consistent with the XRD results. Besides, the O-H vibration shifted from 3243 to 3297 cm⁻¹, and the peak strength was significantly weakened, which is due to ion exchange between H⁺ of O-H group and Cd(II). Likewise, the Ti-O(TiO(OH)2) vibration at 881 cm⁻¹ disappeared for 2-CP- and Cd(II)-laden TNTs@AC from the binary systems. Meanwhile, the O-H vibration shifted from 3243–3240 cm⁻¹, and the peak intensity decreased sharply, which can be caused by the interference of the characteristic peak of phenol. Moreover, the H-O-H vibration shifted from 1629 to 1616 cm⁻¹, and the peak intensity decreased sharply due to the reduction of the bound water. In summary, the adsorption mechanism in the binary solute systems is the same as in the single-solute systems.

The surface elemental compositions of TNTs@AC before and after reaction with Cd(II) and/or 2-CP were further investigated by XPS. Fig. 8a and Table S2 give the near-surface atomic compositions. TNTs@AC before reaction was mainly composed of C (18.13%), O (64.30%), Na (8.61%), and Ti (8.96%). After reacting with Cd(II), the ratio of Cd on the surface increased from 0% to 2.90%, while the ratio of Na on the surface decreased from 8.61% to 0, which is in accord with the ion exchange mechanism. After reacting with 2-CP, the ratio of Cl and C on the surface increased from 0, 18.13% to 0.08, 31.83%, respectively. After sorption of both Cd(II) and 2-CP, the ratio of Na, C, Cl and Cd on the surface changed from 8.61%, 18.13%, 0, 0–0, 45.49%, 0.31% and 0.73%, respectively, where the disappearance of Na and the appearance of Cd were consistent with the mechanisms in the single-solute systems.

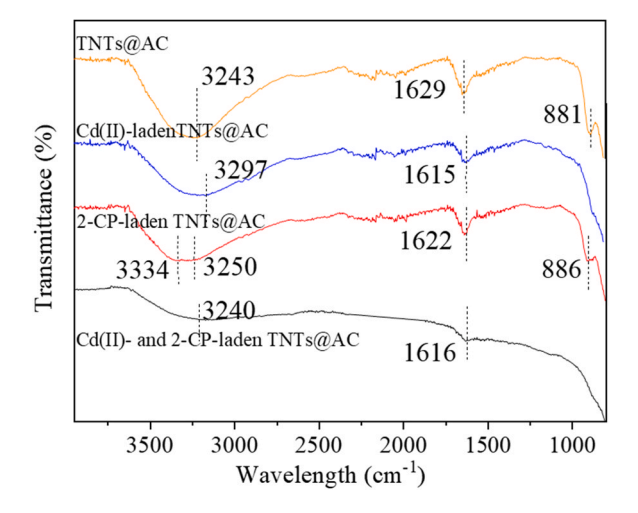


Fig. 7. FTIR spectra of TNTs@AC, Cd(II)-laden TNTs@AC, 2-CP-laden TNTs@AC, and Cd(II)- and 2-CP-laden TNTs@AC.

Figs. 8b-8g shows the XPS spectra of C 1 s, O 1 s, Na 1 s, Ti 2p, Cd 3d, and Cl 2p. For neat TNTs@AC, the C 1 s spectra was deconvoluted into three peaks at 284.8 eV, 286.4 eV, and 89.3 eV, which correspond to the characteristics of C-C/C=C (68.06%), C-O (11.62%), and C(O)O (20.32%),[7,13,40,41] respectively. The O 1 s spectra displayed three peaks at 531 eV (84.88%), 533.1 eV (10.22%), and 536.4 eV (4.9%), which are attributed to TiO₆, M-OH/C-OH, and H₂O, [18,20,27] respectively. The peak of M-OH/C-OH represents the Ti-O-C bond, which proves that TNTs and AC are not combined by simple adhesion, but forming a stable chemical bond. The Na 1 s spectra displayed one peak, which is attributed to -ONa at 1071.8 eV (100%) [31]. The Ti 2p spectra showed three peaks at 454.1 eV (61.66%), 459.9 eV (30.50%), and 467.2 eV (7.84%), which are attributed to Ti 2p_{3/2}, Ti 2p_{1/2}, and satellite peak, [36,42,43] respectively.

After reacting with Cd(II), the Cd 3d spectra showed two peaks at 405.7 eV (61.64%) and 412.4 eV (38.36%), which belong to Cd $3d_{5/2}$ and Cd $3d_{3/2}$ [15,44,45], respectively. Both peaks indicate binding of Cd with O, indicating that adsorption of Cd(II) is due to the ion exchange mechanism. The O 1 s spectra at 533.1 eV (M-OH/C-OH) for TNTs@AC shifted to 532.8 eV for Cd(II)-laden TNTs@AC. The intensity of H_2O , M-OH/C-OH, and TiO_6 changed from 4.9%, 10.22%, 84.88% for TNTs@AC to 0, 13.32% and 86.68% for Cd(II)-laden TNTs@AC. These changes are attributed to adsorption of Cd(II), which introduced the Cd-O group and removed the binding water in TNTs@AC. The Na 1 s spectra at 1071.8 eV (-ONa) almost disappeared.

After reacting with 2-CP, Cl 2p spectra exhibited two peaks at 198.9 eV (34.3%) and 200 eV (63.7%), which are due to M-Cl and C-Cl, respectively. The C 1 s spectra at 289.3 eV (C(O)O) and 286.4 eV (C-O) for TNTs@AC shifted to 289.5 eV and 286.8 eV for 2-CP-laden TNTs@AC. Meanwhile, the intensity of C(O)O, C-O, and C-C/C=C changed from 20.32%, 11.62%, 68.06% for TNTs@AC to 10.38%, 17.13%, 72.49% for 2-CP-laden TNTs@AC. These changes are attributed to the adsorption of 2-CP, which introduced the C-O and C-C/C=C groups.

Upon adsorption of both Cd(II) and 2-CP, the C 1 s spectra at 289.3 eV (C(O)O) for TNTs@AC disappeared while the peak of C=O (12.3%) appeared at 287.4 eV. [46] The intensity of C-O and C-C/C=C increased from 11.62% and 68.06% for TNTs@AC to 14.25% and 73.38% for 2-CP- and Cd(II)-laden TNTs@AC, respectively. The increase of the intensity of C-C/C=C is attributed to the adsorption of 2-CP. The disappearance of C(O)O and the appearance of C=O indicate that the -COOH group was involved in the adsorption process and transformed into C=O or C-O. The peak position and peak intensity of Ti almost did not change after adsorption, and thus the Ti-related groups did not participate in the adsorption reactions.

Based on the above analysis, the possible sorption mechanisms of Cd (II) and 2-CP by TNTs@AC in the single-solute and binary systems are proposed. In the single-solute system, the sorption of Cd(II) is attributed ion exchange between -ONa/-OH groups and Cd(II) (Eqs. 7–8). The adsorption of 2-CP was dominated by hydrophobic interaction and possibly other interactions such as surface complexation and hole filling into the AC-modified TNTs. In the binary systems, the adsorption sites of Cd(II) and 2-CP are different, the presence of 2-CP has little effect on the adsorption of Cd(II), while the adsorption of 2-CP is affected by its own concentration when Cd(II) coexists.

$$Cd^{2+} + (NaO)_2 \equiv Ti_3O_7 \rightarrow CdO_2 \equiv Ti_3O_7 + 2Na^+$$
 (7)

$$Cd^{2+} + (HO)_2 \equiv Ti_3O_7 \rightarrow CdO_2 \equiv Ti_3O_7 + 2H^+$$
 (8)

3.6. Effects of pH, co-existing ions, and HA

3.6.1. Effects of pH

Since pH can affect both the speciation of contaminants and sorbent surface potential, the adsorption of Cd(II) or 2-CP by TNTs@AC is expected to be pH-dependent. Fig. 9a shows that the Cd(II) uptake was

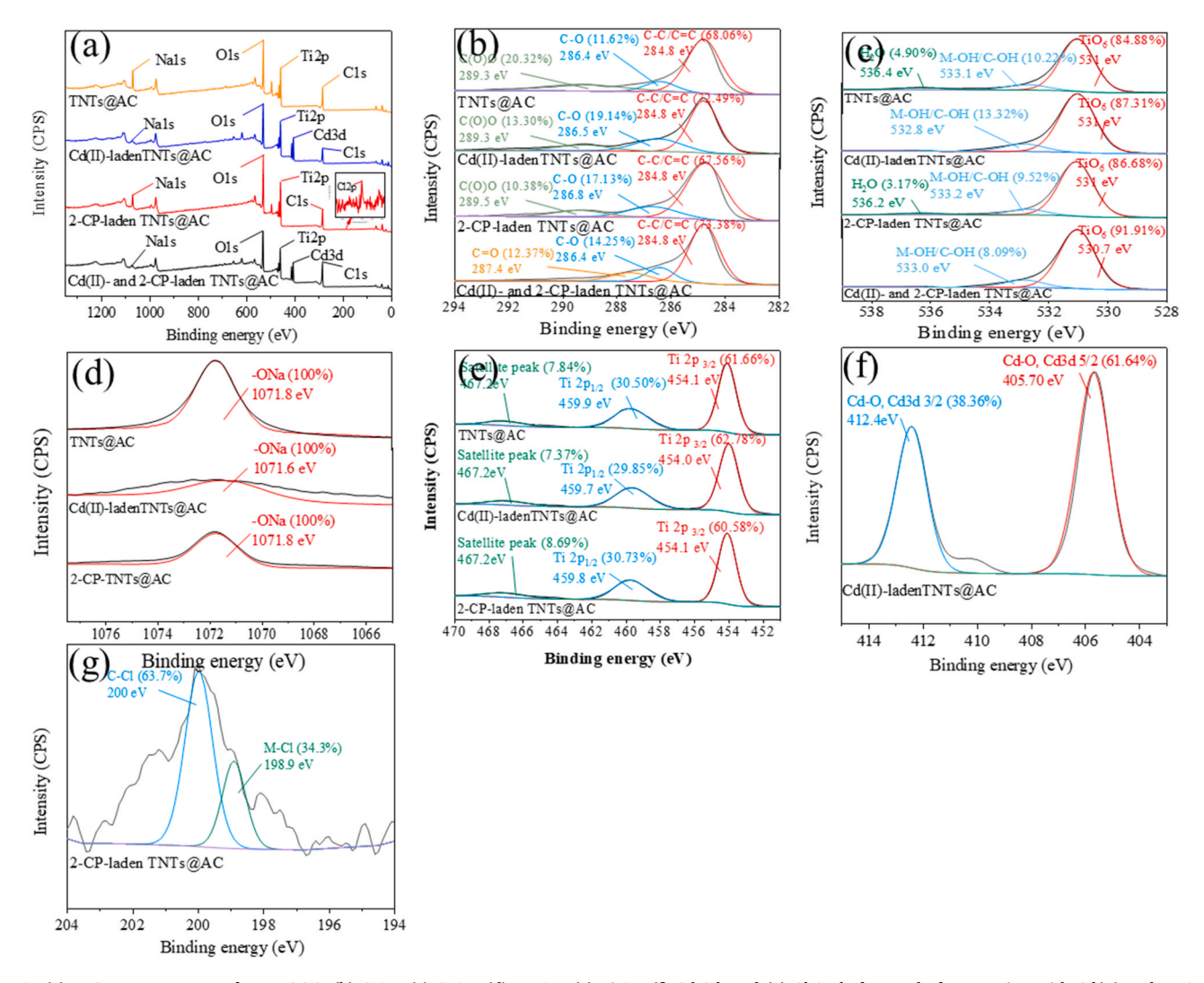


Fig. 8. (a) XPS survey spectra of TNTs@AC, (b) C 1 s, (c) O 1 s, (d) Na 1 s, (e) Ti 2p, (f) Cd 3d, and (g) Cl 2p before and after reaction with Cd(II) and/or 2-CP.

enhanced from 18.6 to 110 mg/g, when the pH was increased from 2.0 to 7.0, respectively. The uptake remained constant at about 110 mg/g at pH 8.0. As shown in Fig. S3, the pH of zero point charge of TNTs@AC was determined to be 2.5. When pH was increased from 2.0 to 3.0, the zeta potential of TNTs@AC was changed from 2.0 mV to -30.1 mV. When pH was further increased from 3.0 to 8.5, the zeta potential was changed from -30.1 to -46.2 mV. Namely, the surface potential turned more negative with increasing pH in the tested pH range (2.0–8.0), which is more favorable for the adsorption of Cd(II).[47].

Unlike Cd(II), the 2-CP uptake remained constant at 38 mg/g over the pH range of 2.0–8.0, and then gradually decreased to 18.7 mg/g at pH 11. The pKa value of 2-CP is 8.52 [20,48]. At pH ≤ 8.0 , the predominant species of 2-CP is the protonated form and the hydrophobic interaction between 2-CP and TNTs@AC is independent of pH. Yet, at elevated pH, 2-CP is deprotonated and negatively charged. The adsorption is then inhibited due to the electrostatic repulsion between 2-CP and negatively charged TNTs@AC. In addition, the hydrophobicity of 2-CP and the material surface is likely reduced with the increasing pH due to the increase polarity [20].

3.6.2. Effects of co-existing ions

Fig. 9b compares the Cd(II) uptakes by TNTs@AC in the presence of NaCl, NaH $_2$ PO $_4$, NaNO $_3$, or CaCl $_2$ (0–10 mM). These cations and anions have been known to be commonly present in natural waters. The addition of co-existing ions inhibited the Cd(II) uptake to various extents. For

instance, increasing the NaCl concentration from 0 to 10 mM inhibited the Cd(II) uptake from 104 to 94.9 mg/g (a 8.99% reduction), whereas increasing CaCl $_2$ from 0 to 10 mM suppressed the Cd(II) uptake from 104 to 44.6 mg/g (a 57.2% reduction). It is evident that the presence of divalent Ca $^{2+}$ showed a stronger inhibiting effect. The presence of cations can directly compete with Cd(II) for sorption sites of TNTs@AC [18], whereas the anionic ligands can form soluble complexes with Cd(II)[47], weakening the interactions between Cd(II) and TNTs@AC.

In contrast, the presence of NaCl, NaH_2PO_4 , and $NaNO_3$ (0–10 mM) improved the 2-CP uptake by 26.6% (38.3–48.5 mg/g), 15.0% (38.3–44.1 mg/g), and 10.0% (38.3–42.2 mg/g), respectively (Fig. 9c). The elevated uptake of 2-CP can be attributed to with the increased ionic strength, which induces the "salting-out" effect. [6].

3.6.3. Effect of HA

Increasing the HA concentration from 0 to 10 mg/L (as TOC) enhanced the Cd(II) uptake from 93.3 to 107 mg/g (a 15.0% enhancement) (Fig. 9d). HA can affect Cd(II) uptake in two contrasting ways. First, HA can complex with Cd(II) via functional groups such as –COOH and –NH₂[49] in the aqueous phase, inhibiting Cd(II) sorption. Second, HA can be adsorbed onto TNTs@AC through complexation between carboxyl and phenolic groups of HA and Ti, hydrophobic interaction, π - π interaction, polar/electrostatic interaction, and hydrogen bonding with AC, [50] and the immobilized HA can serve as a bridge to facilitate binding Cd(II) by forming TNTs@AC-HA-Cd ternary complexes[20].

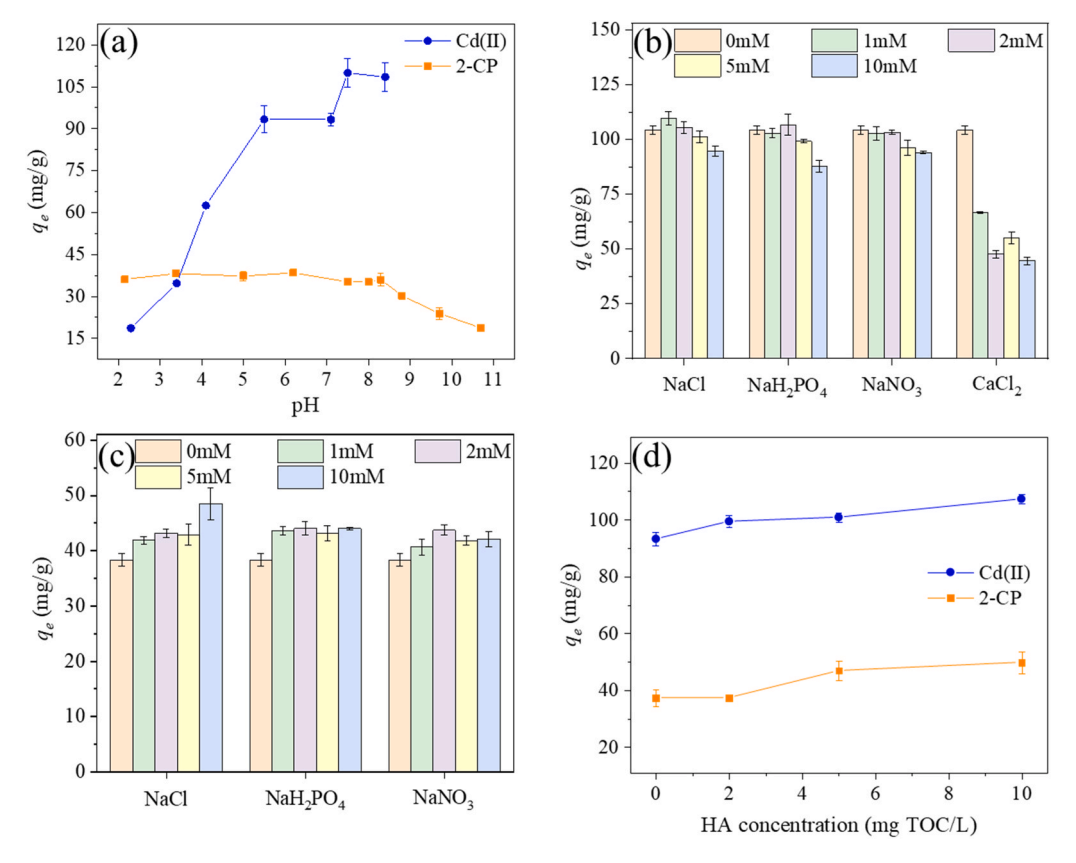


Fig. 9. Effects of (a) pH, (b, c) co-existing ions (b for Cd(II) and c for 2-CP), and (d) HA on equilibrium uptakes of Cd(II) and 2-CP by TNTs@AC in single solute systems. Experimental conditions: initial concentration of Cd(II) or 2-CP = 10 and 5 mg/L, respectively, material dosage = 70 mg/L, pH = 7.0 ± 0.1 , and reaction time = 6 h.

From the experimental data, the facilitating effect of HA outperformed the inhibiting effect.

Similarly, the presence of HA promoted the adsorption of 2-CP (Fig. 9d). As the HA concentration was increased from 0 to 10 mg/L, the 2-CP uptake was enhanced from 37.3 to 49.8 mg/g (a 33.5% increase). The adsorbed HA on TNTs@AC can inhibit the surface potential of the material and enhance its hydrophobicity,[20] In addition, the phenolic group of 2-CP can interact with the carboxyl and hydroxyl groups of HA through hydrogen bonding leading to enhanced sorption of 2-CP.

4. Conclusions

A composite material was synthesized through a simple one-step hydrothermal method using commercially available TiO2 and AC, and investigated for simultaneous removal of Cd(II) and 2-CP from aqueous solution. In the mixed TNTs and AC phases, TNTs was responsible for taking up Cd(II), whereas AC for 2-CP. As such, the relative adsorption capacities of the composite for Cd(II) and 2-CP varied with the mass ratio of TiO2:AC, with decent uptakes for both chemicals in the mass ratio range of 1:3 \sim 1:1. In practice, the mass ratio can be easily adjusted according to the relative contents of the cantaminants in water. TNTs@AC demonstrated excellent sorption capacities for Cd(II) and 2-CP in both single-solute and binary systems. The classical Langmuir model well fitted the adsorption isotherms for Cd(II), whereas the Dualmodel model best interreted the 2-CP adsorption isotherms, and the maximum monolayer adsorption capacity reached 109 mg/g for Cd(II) and 52 mg/g for 2-CP. The dominant adsorption mechanism of Cd(II) was the ion exchange between Cd(II) and Na⁺/H⁺ of the -ONa/H group, while 2-CP was removed via hydrophobic interaction. Increasing pH enhanced the Cd(II) uptake, while the 2-CP uptake remained constant.

The presence of co-existing ions (up to 10 mM), such as Na⁺, Ca²⁺, Cl⁻, NO₃, and H₂PO₄, inhibited Cd(II) uptake, but enhanced the 2-CP uptake. The presence of HA improved the sorption of both Cd(II) and 2-CP.

TNTs@AC holds the potential to be employed as an effective sorbent for removal of both metal cations and hydrophobic organic pollutants from contaminated water. Given the photocatalytic capability of TNTs@AC, the adsorbed organic matter may be degraded udner UV light, which automatically regenerates the material. The adsorbed metals may be desorbed and recovered using a regenerant (e.g., brine or NaCl) commonly used for ion exchange resins. The regernation and solid-phgase photodegration are to be investigated in the next phase.

CRediT authorship contribution statement

Xianping Deng: Methodology, Validation, Data curation, Writing. Peiwen Wu: Writing – review & editing. Xiaodong Du: Writing – review & editing. Guining Lu: Supervision. Yanyan Gong: Writing – review & editing, Data curation, Supervision. Zhi Dang: Supervision. Dongye Zhao: Writing – review & editing, Data curation, Supervision.

Declaration of Competing Interest

The authors declare that they have no known competing financial interests or personal relationships that could have appeared to influence the work reported in this paper.

Data Availability

Data will be made available on request.

Acknowledgments

This study was supported by the National Natural Science Foundation of China (No. 41931288), the US National Science Foundation (CBET-2041060), the Local Innovation and Entrepreneurship Team Project of Guangdong Special Support Program (No. 2019BT02L218), and Guangdong Science and Technology Program (No. 2019B110207001).

Appendix A. Supporting information

Supplementary data associated with this article can be found in the online version at doi:10.1016/j.colsurfa.2023.131756.

References

- [1] K. Wei, K. Li, Z. Zeng, et al., Synergistic photocatalytic effect of porous g-C3N4 in a Cr(VI)/4-chlorophenol composite pollution system, Chin. J. Catal. 38 (2017) 1804–1811.
- [2] A. Chen, G. Zeng, G. Chen, et al., Novel thiourea-modified magnetic ion-imprinted chitosan/TiO2 composite for simultaneous removal of cadmium and 2,4dichlorophenol, Chem. Eng. J. 191 (2012) 85–94.
- [3] Z. Huang, G. Chen, G. Zeng, et al., Polyvinyl alcohol-immobilized Phanerochaete chrysosporium and its application in the bioremediation of composite-polluted wastewater, J. Hazard. Mater. 289 (2015) 174–183.
- [4] Y. Gong, Y. Liu, J. Shen, et al., Simultaneous removal of atrazine and heavy metal ions using sulfonated polymeric microspheres through an adsorptive filtration process: insights into the synergistic and competitive adsorption, J. Clean. Prod. 358 (2022), 132046.
- [5] T.O. Ajiboye, O.A. Oyewo, D.C. Onwudiwe, Simultaneous removal of organics and heavy metals from industrial wastewater: a review, Chemosphere 262 (2021), 128270
- [6] Z. Zhang, X. Hou, X. Zhang, et al., The synergistic adsorption of pyrene and copper onto Fe(III) functionalized mesoporous silica from aqueous solution, Colloids Surf. A: Physicochem. Eng. Asp. 520 (2017) 39–45.
- [7] J. Deng, X. Zhang, G. Zeng, et al., Simultaneous removal of Cd(II) and ionic dyes from aqueous solution using magnetic graphene oxide nanocomposite as an adsorbent, Chem. Eng. J. 226 (2013) 189–200.
- [8] Z.N. Garba, W. Zhou, I. Lawan, et al., An overview of chlorophenols as contaminants and their removal from wastewater by adsorption: a review, J. Environ. Manag. 241 (2019) 59–75.
- [9] P.T. Gauthier, W.P. Norwood, E.E. Prepas, et al., Metal-PAH mixtures in the aquatic environment: a review of co-toxic mechanisms leading to more-than-additive outcomes, Aquat. Toxicol. 154 (2014) 253–269.
- [10] L. Ma, Y. Xi, H. He, et al., Efficiency of Fe-montmorillonite on the removal of Rhodamine B and hexavalent chromium from aqueous solution, Appl. Clay Sci. 120 (2016) 9-15
- [11] G. Yang, L. Tang, G. Zeng, et al., Simultaneous removal of lead and phenol contamination from water by nitrogen-functionalized magnetic ordered mesoporous carbon, Chem. Eng. J. 259 (2015) 854–864.
- [12] S. Andini, R. Cioffi, F. Montagnaro, et al., Simultaneous adsorption of chlorophenol and heavy metal ions on organophilic bentonite, Appl. Clay Sci. 31 (2006) 126–133.
- [13] Y. Ma, H. Li, C. Xie, et al., Treatment of PBDEs from soil-washing effluent by granular-activated carbon: adsorption behavior, Influ. Factors Density Funct. Theory Calc. Process. 10 (9) (2022) 10091815.
- [14] N. Wibowo, L. Setyadhi, D. Wibowo, et al., Adsorption of benzene and toluene from aqueous solutions onto activated carbon and its acid and heat treated forms: influence of surface chemistry on adsorption, J. Hazard Mater. (1-2) (2007) 237-242
- [15] M. Fan, J. Wang, H. Gao, et al., Surface functionalization of activated carbon and adsorption property of cadmium ion, Appl. Chem. Ind. 51 (2022) 1976–1978+ 1984.
- [16] W. Liu, T. Wang, A.G. Borthwick, et al. Adsorption of Pb2+, Cd2+, Cu2+ and Cr3+ onto titanate nanotubes: competition and effect of inorganic ions. Science of the Total Environment, 456–457 (2013) 171–180.
- [17] H. Meng, W. Hou, X. Xu, et al., TiO2-loaded activated carbon fiber: hydrothermal synthesis, adsorption properties and photo catalytic activity under visible light irradiation, Particuology 14 (2014) 38–43.
- [18] W. Liu, X. Zhao, T. Wang, et al., Adsorption of U(VI) by multilayer titanate nanotubes: effects of inorganic cations, carbonate and natural organic matter, Chem. Eng. J. 286 (2016) 427–435.
- [19] Y. Zhu, T. Xu, D. Zhao, et al., Adsorption and solid-phase photocatalytic degradation of perfluorooctane sulfonate in water using gallium-doped carbonmodified titanate nanotubes, Chem. Eng. J. 421 (2021), 129676.
- [20] J. Duan, H. Ji, T. Xu, et al., Simultaneous adsorption of uranium(VI) and 2-chlor-ophenol by activated carbon fiber supported/modified titanate nanotubes (TNTs/ACF): Effectiveness and synergistic effects, Chem. Eng. J. 406 (2021), 126752.
- [21] Y. Ge, I. Akpinar, Z. Li, et al., Porous structured cotton-based ACF for the adsorption of benzen, Chemosphere 282 (2021), 131110.

- [22] Q. Wang, X. Lei, F. Pan, et al., A new type of activated carbon fibre supported titanate nanotubes for high-capacity adsorption and degradation of methylene blue, Colloids Surf. A: Physicochem. Eng. Asp. 555 (2018) 605–614.
- [23] Y. Li, Y.Chuan Simultaneous, As(III) and Cd removal and recovery from copper smelting wastewater (in China), China Acad. J. Electron. Publ. House 52 (2014).
- [24] Liuzhou wood treatment plant containing oil, phenol, five Monitoring report on treatment effect of phenol industrial wastewater. Railway Labour Health Bulletin, 02 (1981) 21–24.
- [25] D. Eeshwarasinghe, P. Loganathan, S. Vigneswaran, Simultaneous removal of polycyclic aromatic hydrocarbons and heavy metals from water using granular activated carbon, Chemosphere 223 (2019) 616–627.
- [26] F. Li, Z. Wei, K. He, et al., A concentrate-and-destroy technique for degradation of perfluorooctanoic acid in water using a new adsorptive photocatalyst, Water Res. 185 (2020), 116219.
- [27] X. Zhao, Z. Cai, T. Wang, et al., A new type of cobalt-deposited titanate nanotubes for enhanced photocatalytic degradation of phenanthrene, Appl. Catal. B: Environ. 187 (2016) 134–143.
- [28] J. Ma, F. Li, T. Qian, et al., Natural organic matter resistant powder activated charcoal supported titanate nanotubes for adsorption of Pb(II), Chem. Eng. J. 315 (2017) 191–200.
- [29] L. Xiong, C. Chen, Q. Chen, et al., Adsorption of Pb(II) and Cd(II) from aqueous solutions using titanate nanotubes prepared via hydrothermal method, J. Hazard. Mater. 189 (3) (2011) 741–748.
- [30] K.S.W. SING, D.H. EVERETT, R.A.W. HAUL, et al., Reporting physisorption data for gas/solid systems with special reference to the determination of surface area and porosity, Pure Appl. Chem. 57 (1985) 603–619.
- [31] L. Zhang, X. Wang, H. Chen, et al., Adsorption of Pb(II) using magnetic titanate nanotubes prepared via two-step hydrothermal method, CLEAN - Soil Air Water 42 (7) (2014) 947–955.
- [32] H. Yu, J. Yu, B. Cheng, et al. Synthesis, characterization and photocatalytic activity of mesoporous titania nanorod/titanate nanotube composites. Journal of Hazardous Materials, 147(1–2) (2007) 581–587.
- [33] G.M. Walker, L.R. Weatherley, Adsorption of dyes from aqueous solution the effect of adsorbent pore size distribution and dye aggregation, Chem. Eng. J. 83 (2001) 201–206.
- [34] M.I. Konggidinata, B. Chao, Q. Lian, et al., Equilibrium, kinetic and thermodynamic studies for adsorption of BTEX onto Ordered Mesoporous Carbon (OMC), J. Hazard. Mater. 336 (2017) 249–259.
- [35] R. Shahrokhi-Shahraki, P.S. Kwon, J. Park, et al., BTEX and heavy metals removal using pulverized waste tires in engineered fill materials, Chemosphere 242 (2020), 125281.
- [36] K. Cheng, Z. Cai, J. Fu, et al., Synergistic adsorption of Cu(II) and photocatalytic degradation of phenanthrene by a jaboticaba-like TiO2/titanate nanotube composite: an experimental and theoretical study, Chem. Eng. J. 358 (2019) 1155–1165.
- [37] W. Liu, Z. Cai, X. Zhao, et al., High-capacity and photoregenerable composite material for efficient adsorption and degradation of phenanthrene in water, Environ. Sci. Technol. 50 (20) (2016) 11174–11183.
- [38] T. Wang, W. Liu, N. Xu, et al., Adsorption and desorption of Cd(II) onto titanate nanotubes and efficient regeneration of tubular structures, J. Hazard. Mater. 250 (2013) 379–386.
- [39] B. Li, L.J. Ma, Y. Tian, et al., A catechol-like phenolic ligand-functionalized hydrothermal carbon: one-pot synthesis, characterization and sorption behavior toward uranium, J. Hazard. Mater. 271 (2014) 41–49.
- [40] X. Yang, H. Cai, M. Bao, et al., Insight into the highly efficient degradation of PAHs in water over graphene oxide/Ag3PO4 composites under visible light irradiation, Chem. Eng. J. 334 (2018) 355–376.
- [41] Y. Sun, Z. Wu, X. Wang, et al., Macroscopic and microscopic investigation of U(VI) and Eu(III) adsorption on carbonaceous nanofibers, Environ. Sci. Technol. 50 (8) (2016) 4459–4467.
- [42] M. Li, X. Zhang, Y. Liu, et al., Pr3+ doped biphasic TiO2 (rutile-brookite) nanorod arrays grown on activated carbon fibers: hydrothermal synthesis and photocatalytic properties, Appl. Surf. Sci. 440 (2018) 1172–1180.
- [43] H. Ji, W. Liu, F. Sun, et al., Experimental evidences and theoretical calculations on phenanthrene degradation in a solar-light-driven photocatalysis system using silica aerogel supported TiO2 nanoparticles: insights into reactive sites and energy evolution, Chem. Eng. J. 419 (2021), 129605.
- [44] Y. Yu, J. Liu, Y. Yang, et al., Experimental and theoretical studies of cadmium adsorption over Fe2O3 sorbent in incineration flue gas, Chem. Eng. J. 425 (2021), 131647.
- [45] M. Thambidurai, N. Muthukumarasamy, A. Ranjitha, et al., Structural and optical properties of Ga-doped CdO nanocrystalline thin films, Superlattices Microstruct. 86 (2015) 559–563.
- [46] Y. Sun, S. Yang, Y. Chen, et al., Adsorption and desorption of U(VI) on functionalized graphene oxides: a combined experimental and theoretical study, Environ. Sci. Technol. 49 (7) (2015) 4255–4262.
- [47] X. Hua, J. Hu, X. Jiang, et al., Adsorption of Cd to natural biofilms in the presence of EDTA: effect of pH, concentration, and component addition sequence, Environ. Sci. Pollut. Res. 20 (2) (2013) 1079–1088.

- [48] Q. Liu, T. Zheng, P. Wang, et al., Adsorption isotherm, kinetic and mechanism studies of some substituted phenols on activated carbon fibers, Chem. Eng. J. (2010) 348–356.
- [49] T. Wang, W. Liu, L. Xiong, et al., Influence of pH, ionic strength and humic acid on competitive adsorption of Pb(II), Cd(II) and Cr(III) onto titanate nanotubes, Chem. Eng. J., 215- 216 (2013) 366–374.
- [50] M.R. Yazdani, N. Duimovich, A. Tiraferri, et al., Tailored mesoporous biochar sorbents from pinecone biomass for the adsorption of natural organic matter from lake water, J. Mol. Liq. 291 (2019), 111248.